Rapid Communications

Impact of strong anisotropy on the phase diagram of superfluid ^{3}He in aerogels

Tomohiro Hisamitsu, Masaki Tange, and Ryusuke Ikeda
Department of Physics, Graduate School of Science, Kyoto University, Kyoto 606-8502, Japan

(Received 31 January 2020; revised manuscript received 27 February 2020; accepted 28 February 2020; published 12 March 2020)

Recently, one analog of the Anderson's theorem for the *s*-wave superconductor has attracted much interest in the context of the *p*-wave polar pairing state of superfluid ^{3}He in a model aerogel in the limit of strong uniaxial anisotropy. We discuss to what extent the theorem is satisfied in the polar phase in real aerogels by examining the normal to polar transition temperature T_c and the low temperature behavior of the superfluid energy gap under an anisotropy of a moderate strength and comparing the obtained results with experimental data. The situation in which the Anderson's theorem clearly breaks down is briefly discussed.

DOI: 10.1103/PhysRevB.101.100502

Recent observations on superfluid ^{3}He in anisotropic aerogels have clarified profound roles of an anisotropy for the superfluid phase diagram and properties. The polar pairing state [1] has been discovered in nematic aerogels with a nearly one-dimensional structure [2]. It has been found that this polar pairing state does not occur when the magnetic scattering effect due to the solid ^{3}He localized on the surface of the aerogel structure is active [3]. This high sensitivity to the type of "impurity" scatterings of the superfluid phase diagram is not easily explained within the original theoretical model assuming a *weak* global anisotropy of the aerogel structure [1,4].

It has been pointed out that, in the limit of strong anisotropy, i.e., when the orientation of the aerogel strands is perfectly ordered, the normal to polar transition temperature $T_c(P)$ should be insensitive to the (nonmagnetic) impurity scattering strength [5]. Recently, this argument analogous to the Anderson's theorem in the *s*-wave superconductor [6] has attracted much interest [7,8] in relation to the low temperature behavior of the energy gap in the polar phase and to the robustness of the polar phase in relatively dense nematic aerogels. Previously, various features seen in superfluid ^{3}He in nematic aerogels [2,7] have been discussed based on the model assuming the *weak* anisotropy [1]. Once taking account of the puzzling result [3] brought by the magnetic impurities altogether, the approach starting from the side of the strong anisotropy may be more appropriate. Further, the polar phase has been detected so far only in the nematic aerogels where the strands are oriented on average in one direction. Then, one might wonder whether the polar phase occurs only in the limit of strong anisotropy.

In this work, consequences of the strong anisotropy in the phase diagram of superfluid ^{3}He in aerogels with no magnetic scattering effect are studied in detail within the weak-coupling BCS approximation. Throughout the present Rapid Communication, the strength of the anisotropy is assumed to be measured by the size of a correlation length L_z, defined along the averaged orientation of the strands, of the random scattering potential. It is found that the impurity-scattering independent T_c, i.e., the Anderson's theorem [5,6], is approximately satisfied even in the scattering potential model with a finite L_z. Thus, we argue that, consistently with the original argument [1], the polar phase may be realized even in aerogels where the strands' orientation is to some extent disordered. Further, the dependences of the superfluid energy gap $|\Delta(T)|$ on the impurity scattering effect are also examined, and the T^3 behavior arising from the horizontal line node of $|\Delta(T)|$ in the polar pairing symmetry is found to be robust against changes of the impurity strength and the anisotropy. Further, the situation in which $T_c(P)$ is also reduced so that the Anderson's theorem is not satisfied will also be commented on.

First, let us describe how the Anderson's theorem occurs in the context of the *p*-wave superfluid phase in an environment with nonmagnetic elastic impurity scatterings. The starting model of our analysis to be performed below is the BCS Hamiltonian for a spatially uniform equal-spin paired state in zero magnetic field

$$\mathcal{H}_{\rm BCS} - \mu N = \sum_{\mathbf{p},\sigma}\left[\xi_{\mathbf{p}} a^\dagger_{\mathbf{p},\sigma} a_{\mathbf{p},\sigma} - \frac{1}{2}(\Delta^*_{\mathbf{p}} a_{\mathbf{p},\sigma} a_{-\mathbf{p},\sigma} + \text{H.c.})\right] + g^{-1} V|\Delta|^2, \quad (1)$$

where g is the strength of the attractive interaction, V is the system volume, and $\xi_{\mathbf{p}}$ is the quasiparticle energy measured from the Fermi energy μ. Further, $\Delta_{\mathbf{p}}/\Delta$ is the form factor, i.e., the momentum dependence representing the pairing symmetry, and Δ is determined by the gap equation [see Eq. (4)].

The total Hamiltonian $\mathcal{H}$ is the sum of Eq. (1) and the nonmagnetic impurity potential term

$$\mathcal{H}_{\rm imp} = \int d^3\mathbf{r}\, u(\mathbf{r}) n(\mathbf{r}), \quad (2)$$

where $n(\mathbf{r})$ is the particle density operator. As usual, the impurity scattering can be modeled by the correlator

$$W(\mathbf{r}) = 2\pi N(0)\tau \langle u(\mathbf{r}) u(0)\rangle_{\rm imp}, \quad (3)$$

or its Fourier transform $w(\mathbf{k}) = \int d^3\mathbf{r}\, W(\mathbf{r}) e^{i\mathbf{k}\cdot\mathbf{r}}$, with $\langle u\rangle_{\rm imp} = 0$, where $\langle\cdot\rangle_{\rm imp}$ denotes the random average, $\mathbf{k}$ is the momentum transfer, $N(0)$ is the density of states on the Fermi surface per spin in the normal state, and τ is the relaxation time of the normal quasiparticle in the case with no anisotropy. For simplicity, the Born approximation will be used to incorporate the impurity-scattering effect in the Green's functions for the quasiparticles in an equal-spin paired superfluid state. Then, we have a mean-field problem for spinless fermions, and solving the corresponding gap equation can be performed in quite the same manner as in the s-wave paired case [9]. The resulting gap equation can be expressed in the form

$$\ln\left(\frac{T}{T_{c0}(P)}\right) = \pi T \sum_{\varepsilon}\left[\frac{-1}{|\varepsilon|} + 3\left\langle \frac{\Delta_{\mathbf{p}}\tilde{\Delta}_{\mathbf{p}}\Delta^{-2}}{\sqrt{\tilde{\varepsilon}_{\mathbf{p}}^2 + |\tilde{\Delta}_{\mathbf{p}}|^2}}\right\rangle_{\hat{p}}\right], \quad (4)$$

where $\varepsilon = \pi T(2m+1)$ with integer m, $T_{c0}(P)$ is the superfluid transition temperature of the bulk liquid, and $\langle\cdot\rangle_{\hat{p}}$ denotes the angle average on the unit vector $\hat{p}$ over the Fermi surface. Further, in Eq. (4),

$$i\tilde{\varepsilon}_{\mathbf{p}} = i\varepsilon - \frac{1}{2\pi N(0)\tau}\int_{\mathbf{q}} w(\mathbf{p}-\mathbf{q})\mathcal{G}_{\mathbf{q}}(\varepsilon),$$
$$\tilde{\Delta}_{\mathbf{p}} = \Delta_{\mathbf{p}} - \frac{1}{2\pi N(0)\tau}\int_{\mathbf{q}} w(\mathbf{p}-\mathbf{q})[\mathcal{F}_{\mathbf{q}}^{\dagger}(\varepsilon)]^*, \quad (5)$$

and

$$\mathcal{G}_{\mathbf{p}}(\varepsilon) = \frac{-i\tilde{\varepsilon}_{\mathbf{p}} - \xi_{\mathbf{p}}}{\tilde{\varepsilon}_{\mathbf{p}}^2 + \xi_{\mathbf{p}}^2 + |\tilde{\Delta}_{\mathbf{p}}|^2},$$
$$\mathcal{F}_{\mathbf{p}}^{\dagger}(\varepsilon) = \frac{-\tilde{\Delta}_{\mathbf{p}}^*}{\tilde{\varepsilon}_{\mathbf{p}}^2 + \xi_{\mathbf{p}}^2 + |\tilde{\Delta}_{\mathbf{p}}|^2} \quad (6)$$

are the impurity-averaged Matsubara Green's functions [9].

As a model of the impurity correlator (3) in the presence of a stretched anisotropy favoring the polar phase in which $\Delta_{\mathbf{p}} = \Delta\hat{p}_z$, we will use the following expression:

$$W(\mathbf{r}) = \frac{k_{\rm F}}{2}\delta^{(2)}(\mathbf{r}_\perp)\exp(-|z|/L_z) \times[1 + \Theta(1-|\delta_u|)(|\delta_u|^{-1/2} - 1)], \quad (7)$$

where $\Theta(x)$ is the step function, $|\delta_u| = k_{\rm F}^2 L_z^2$, and L_z is the correlation length, defined along the axis of the stretched anisotropy, of the random distribution of the potential $u(\mathbf{r})$. This anisotropy axis corresponds to the averaged orientation of the strands of a nematic aerogel and, hereafter, will be taken as the z axis. The strength of the anisotropy is measured by $|\delta_u|$, while the measure of the impurity strength is $1/(\tau T_{c0})$ [10], where $k_{\rm F}$ is the Fermi wave number. Then, the Fourier transform $w(\mathbf{k})$ of $W(\mathbf{r})$ becomes

$$w(\mathbf{k}) = \frac{\sqrt{|\delta_u|}}{1 + |\delta_u|\hat{k}_z^2}(1 + (|\delta_u|^{-1/2} - 1)\Theta(1 - |\delta_u|)). \quad (8)$$

Equation (8) has the following limiting cases. For the weak anisotropy, $|\delta_u| < 1$, this model reduces to the expression $w(\mathbf{k}) \simeq 1 - |\delta_u|\hat{k}_z^2$, introduced in Ref. [1]. The opposite $L_z \to \infty$ limit of Eq. (8) corresponds to the case with the impurity scattering persistent along the z axis. In this case, $w(\mathbf{k})$ reduces to

$$w_\infty(\mathbf{k}) = \pi k_{\rm F}\delta(k_z), \quad (9)$$

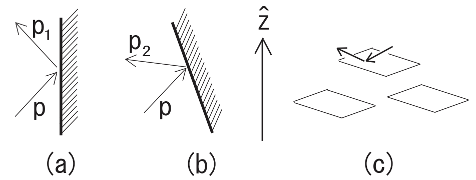

FIG. 1. (a) Description of the specular reflection on the wall parallel to the z axis. That is, the z component of the momentum is conserved. (b) Example showing that the z component of the momentum is not conserved through the reflection on a wall tilted from the z axis. (c) Rough picture of planar scattering centers positioned randomly and with their surface perpendicular to the z axis. On each center, the component perpendicular to the z axis of the momentum is conserved at each scattering event.

implying that, as sketched in Fig. 1(a), the scattering is specular along the z axis. In contrast, if, as in Fig. 1(b), quasiparticles are scattered locally by a wall tilted from the z axis, the correlation length L_z is finite on average. Therefore, the anisotropy in our model (7) is a measure of the orientational ordering of the strands. In fact, L_z in real samples seems to be finite based on the fact that splayed strands and crossings between straight strands are seen in real images of the nematic aerogels [2,8]. We also note that the point of view regarding a tilt of correlated defects with infinite correlation length as a segmented defect with a finite correlation length has been used previously to explain a mysterious sign reversal of the vortex Hall conductivity in superconductors [11]. The model (7) interpolating the above-mentioned two limits has been used to study half-quantum vortex (HQV) pairs in the polar-distorted B (PdB) phase at lower temperatures [12].

The Anderson's theorem for the polar pairing state with $\Delta_{\mathbf{p}} = \Delta\hat{p}_z$ in the perfectly ordered aerogel is easily verified in terms of Eq. (9). In fact, by applying Eq. (9) to Eq. (5), any $1/(\tau T_{c0})$ dependence in the last term of Eq. (4) is canceled between the denominator and numerator of the term, and, as in the s-wave pairing case, the gap equation (4) becomes its expression in clean limit or for the bulk liquid. As argued above, however, a partial deviation from the Anderson's theorem should be present in the polar phase in real aerogels. To clarify this point, the polar to normal transition temperature $T_c(P)$ and the superfluid gap $|\Delta(T)|$ in the polar phase will be numerically examined using Eqs. (4) and (8) for various values of the anisotropy δ_u and the impurity strength $1/(\tau T_{c0})$.

Besides $T_c(P)$, let us determine where the polar phase becomes unstable on cooling. The polar to the polar-distorted A (PdA) transition [1,2,8] is continuous as well as the polar to PdB transition [12], and, in the present weak-coupling approximation, both of them has the *same* transition temperature [13]. Thus, it may be allowed to identify hereafter the polar to PdB transition line $T_{\rm PB}(P)$ with the real polar to PdA transition line. The $T_{\rm PB}(P)$ line is easily obtained according to the diagrams sketched in Fig. 2 representing the gap equation linearized with respect to the order parameter of the PdB state by using the quantities characterizing the polar pairing state. Then, $T_{\rm PB}$ is given by the temperature T satisfying

$$\ln\left(\frac{T}{T_{c0}(P)}\right) = \pi T \sum_{\varepsilon}\left[\frac{-1}{|\varepsilon|} + \frac{3}{2}\left\langle \frac{1-\hat{p}_z^2}{\sqrt{\tilde{\varepsilon}_{\mathbf{p}}^2 + |\tilde{\Delta}_{\mathbf{p}}|^2}}\right\rangle_{\hat{p}}\right]. \quad (10)$$

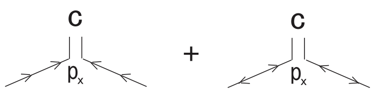

FIG. 2. Diagrams expressing the gap equation linearized with respect to the order parameter of the PdB phase. The parameter c means the order parameter of the PdB phase, and each vertex carries a component perpendicular to the z axis of the momentum. The impurity-averaged Green's functions $\mathcal{G}$ and $\mathcal{F}^\dagger$ in Eq. (6) are indicated by a line with a double arrow and that with a left-right arrow, respectively.

Examples of the $T_c(P)$ and $T_{\rm PB}(P)$ obtained numerically from Eqs. (4) and (10) are presented in Fig. 3, where the experimental data on $T_{c0}(P)$ [14] were used. As is seen in Fig. 3(a) where a moderately large anisotropy $|\delta_u| = 30$ is used in common, $T_c(P)$ weakly depends on the impurity strength τ^{-1}. In general, for a stronger anisotropy, the τ^{-1} dependence of T_c becomes weaker, while the corresponding one of $T_{\rm PB}$ becomes stronger. At higher pressures, the pressure dependence of $T_c/T_{c0}(P)$ is quite weak, reflecting the proximity to the limit of strong anisotropy in which the Anderson's theorem is satisfied, while T_c/T_{c0} is lowered at low enough P values because of an increase of the dimensionless impurity strength $1/[\tau T_{c0}(P)]$. In contrast to T_c, however, $T_{\rm PB}$ is quite sensitive to the impurity strength and rapidly decreases with increasing $1/(\tau T_{c0})$ [5,7]. Thus, the temperature range of the polar phase is wider for a lower P.

Further, as the solid and dashed curves in Fig. 3(b) show, an increase of the anisotropy extends the region of the polar phase: With increasing the anisotropy $|\delta_u|$, T_c is increased and approaches T_{c0}. On the other hand, $T_{\rm PB}$ decreases with increasing the anisotropy. In fact, the $T_{\rm PB}$ values corresponding to the red open circle data of $T_c(P)$ in Fig. 3(b) are almost zero so that the superfluid phase is in the polar pairing state everywhere (see below). In such a manner, the temperature range of the polar phase at a fixed P becomes wider with increasing the anisotropy and/or the impurity strength.

The red open circle symbols, obtained in terms of $(2\pi\tau)^{-1} = 1$ (mK) and $|\delta_u| = 100$, in Fig. 3(b) express the $T_c(P)$ curve comparable with the data for nafen-243 in Ref. [2]. Similarly, we have obtained a curve (not shown in the figures) comparable with the data for nafen-90 [2] in terms of $(2\pi\tau)^{-1} = 0.15$ (mK) and $|\delta_u| = 20$. By reasonably assuming that, in aerogels, a lower porosity would result in an enhancement of $(\tau T_{c0})^{-1}$ measuring the scattering strength due to the aerogel structure [3,15], and that a sample anisotropy should be reflected as an anisotropy on the quasiparticle mean free paths [7], it is found that these correspondences between the experimental data and the present results are qualitatively satisfactory.

Next, as another quantity related to the Anderson's theorem, let us examine the temperature dependence of the energy gap $|\Delta(T)|$ of quasiparticles in the polar phase. As indicated elsewhere [8], the energy gap difference $|\Delta(0)| - |\Delta(T)|$ estimated from the NMR frequency data in the polar phase at 29.5 (bars) is proportional to T^3, reflecting the presence of a line node in $|\Delta(T)|$. Since the relevant energy scale at low T is not T_c but $|\Delta(0)|$, we will express the T^3 behavior

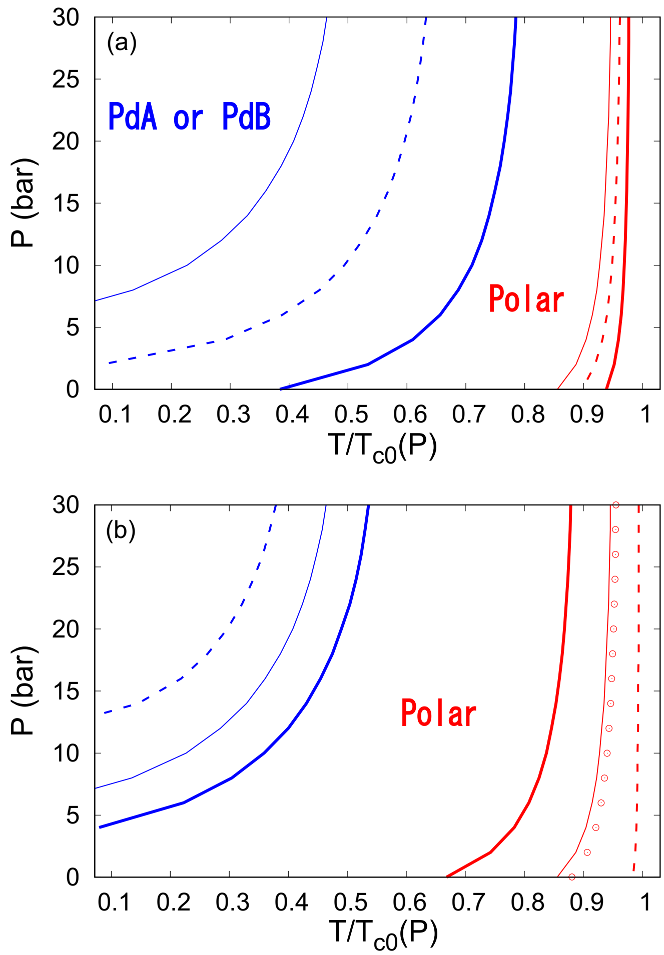

FIG. 3. (a) Dependence of the pressure (P) vs temperature (T) superfluid phase diagram on the impurity strength τ^{-1} under a fixed magnitude of the anisotropy $|\delta_u| = 30$, i.e., $k_{\rm F}L_z = 5.48$. The temperatures $T_c(P)$ (red) and $T_{\rm PB}(P)$ (blue) obtained in terms of the same set of τ^{-1} and $|\delta_u|$ are represented by the same line type or symbol. The thick solid line, the dashed line, and the thin solid curves are the results for $(2\pi\tau)^{-1}$ (mK) = 0.3, 0.5, and 0.7, respectively. Note that the variable of the horizontal axis is $T/T_{c0}(P)$, i.e., the temperature normalized by the bulk superfluid transition temperature T_{c0} at each P. (b) Dependence of the two transition curves on the anisotropy $|\delta_u|$ at a fixed impurity strength $(2\pi\tau)^{-1}$ (mK) = 0.7 (solid and dashed curves). The thin solid curves are the same as in (a), and the thick solid curves are T_c (red) and $T_{\rm PB}$ (blue) for $|\delta_u| = 4.4$. The dashed red and blue curves follow from the $|\delta_u| = 3 \times 10^3$ value which is close to the limit of strong anisotropy. The red open circles obtained in terms of $(2\pi\tau)^{-1}$ (mK) = 1.0 and $|\delta_u| = 100$ are comparable with the $T_c(P)$ data of nafen-243 [2]. The corresponding $T_{\rm PB}[P = 30$ (bars)] value, $0.002T_{c0}$, is not shown in the figure.

in the form

$$1 - \frac{|\Delta(T)|}{|\Delta(0)|} = \bar{a}\frac{T^3}{|\Delta(0)|^3}. \tag{11}$$

This relation to be satisfied in the polar phase in aerogels would indicate that, irrespective of the presence of the impurity scattering effect, the line node of $|\Delta(T)|$ in the polar

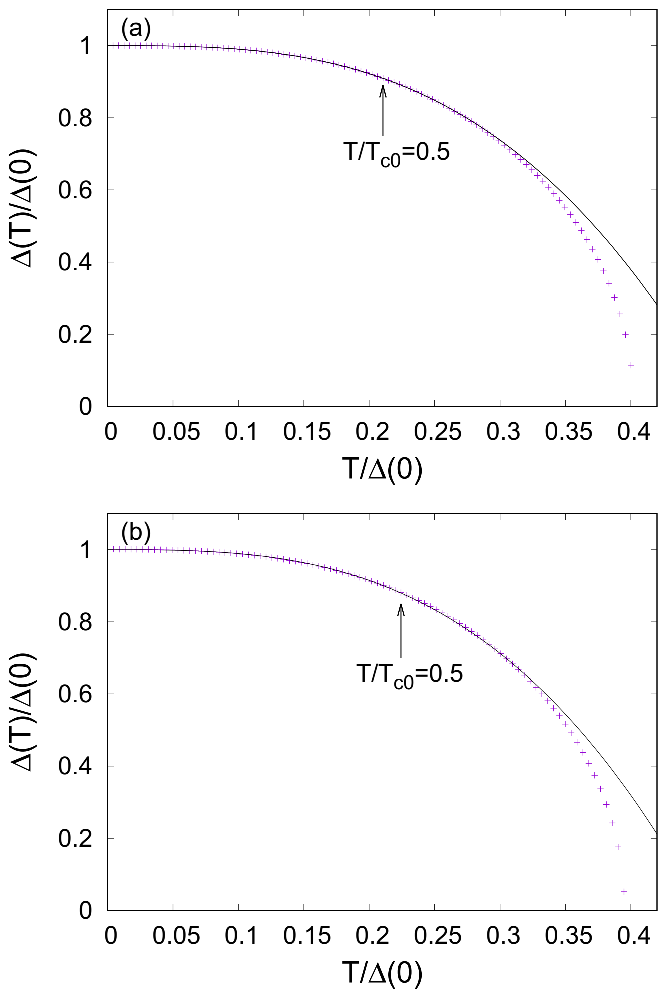

FIG. 4. Temperature dependence of $|\Delta|$ (symbols) obtained in terms of the parameter values $|\delta_u| = 100$ and $(2\pi\tau)^{-1} = 1$ (mK) (a) at 30 (bars) and (b) at 0 (bars), respectively. For comparison, the curves (thin solid curves) obtained by substituting $\overline{a} = 9.70$ for (a) and 10.64 for (b) into Eq. (11) are also drawn. In both cases, the T^3 behavior is nicely seen at least in the range $T < 0.65T_c$. (Note that, in the figures, the temperature is represented in units of $|\Delta(0)|$ in each case.)

phase remains well defined. According to the *calculation* [8] in the weak-coupling approximation and clean limit, the coefficient $\overline{a}$ takes the value 8.49, while the estimated $\overline{a}$ value taken from NMR data in a nematic aerogel at 29.5 (bars) was $0.38[\Delta(0)/T_c]^3$ [8]. According to Ref. [8], this estimated coefficient may become comparable [8] with the weak-coupling value 8.49 in the limit of strong anisotropy if the strong-coupling effect [14] enhancing $|\Delta(0)|$ is taken into account. In a strongly anisotropic case, $|\delta_u| = 3 \times 10^3$, we have obtained the value $\overline{a} = 8.97$ comparable with the weak-coupling value mentioned above.

In Fig. 4, our results (symbols) obtained consistently with the red open circle data in Fig. 3(b), i.e., for the values $(2\pi\tau)^{-1} = 1$ (mK) and $|\delta_u| = 100$, are shown and are fitted to an appropriate T^3 curve (thin solid curve) at a high pressure [30 (bars)] (a) and a low pressure [0 (bars)] (b), respectively. The T^3 behavior is well defined in $T < 0.65T_{c0}$ irrespective of the pressure value, and the effects of the impurity strength and the anisotropy value are exclusively reflected in the coefficient $\overline{a}$ of the T^3 term. As mentioned in the caption of Fig. 4, the $\overline{a}$ value is enhanced especially at lower pressures, reflecting the fact that the impurity effect is stronger as the pressure is lowered. This increase of $\overline{a}$ value for a larger $(\tau T_{c0})^{-1}$ should be expected because $|\Delta|$ should decrease in a more impure case as far as L_z is finite. If the strong-coupling effect is taken into account, according to Ref. [8] the coefficient $a \equiv \overline{a}[T_c/\Delta(0)]^3$ at 29.5 (bars) would remarkably decrease so that the estimated value $a = 0.38$ [8] may be explained. At zero pressure, however, the strong-coupling effect is not effective so that the coefficient a of the T^3 behavior at lower pressures should show a large value of order unity. Hence, examining the T^3 term of the energy gap at low pressures may become a test for the present theory.

It is valuable to point out that the p-wave Anderson's theorem on the superfluid transition temperature is also satisfied in the case of a normal to (distorted) A phase transition under planelike defects with no two-dimensional momentum transfer [see Fig. 1(c)] if the **l** vector of this A phase is oriented along the normal of the plane of the defects. In fact, when the bare pairing vertex is $p_k(\delta_{j,k} - \hat{z}_j\hat{z}_k)$, and Eq. (9) is replaced by the form proportional to $\delta(\hat{k}_x)\delta(\hat{k}_y)$, the superfluid transition temperature resulting from Eq. (4) becomes T_{c0} irrespective of the strength of the impurity scattering. In principle, such a situation can be realized in planar aerogels and would result in an extension of the temperature width of the distorted A phase region at *lower* pressures and hence, according to Ref. [16], in a realization of HQVs in the chiral A phase.

An extension of the present study should be developed to investigate the corresponding response and dynamical properties, because the absence of the impurity scattering effect in the limit of strong anisotropy no longer holds for the gradient energies [17]. On the other hand, we note that the $T_c(P)$ data of the nafen-910 in Ref. [3] showing a remarkable suppression from $T_{c0}(P)$ in spite of the presence of the polar phase cannot be explained within the present theory. As is well known in the context of the dirty s-wave superconductors, the Anderson's theorem itself breaks down due to the impurity scattering effect enhanced further through the repulsive channels of the quasiparticle interaction [18]. If this mechanism is effective, the τ^{-1} dependence of $T_c(P)$ of the type seen in Fig. 3(a) should be seen even in the systems with infinite L_z. It is likely that the remarkably suppressed $T_c(P)$ in the nafen-910 [3] mentioned above is a reflection of this interaction-induced mechanism. To clarify to what extent this interaction effect is relevant to real systems, further comparison between the theory and experimental data would be necessary in the future.

In relation to the robustness of the polar phase against the anisotropic nonmagnetic scatterings studied here, we note that a generalized Anderson's theorem has been discussed theoretically for an interorbital and spin-triplet paired state [19] and an unconventional s-wave paired state [20], and that unexpectedly weak impurity effects on superconductivity in Dirac semimetals and other unconventional multiorbital superconductors have been addressed experimentally [21].

In conclusion, we have investigated to what extent the Anderson's theorem is satisfied in the polar phase by assuming the correlation length of the random potential in nematic aerogels to be long but finite. It has been found that the low temperature behavior of the superfluid energy gap stemming from the presence of the horizontal line node is robust against the impurity scattering and that the resulting phase diagram is qualitatively consistent with the available experimental data.

R.I. is grateful to Vladimir Dmitriev and Bill Halperin for useful discussions. The present work was supported by JSPS KAKENHI (Grant No. 16K05444).

[1] K. Aoyama and R. Ikeda, Phys. Rev. B **73**, 060504(R) (2006).
[2] V. V. Dmitriev, A. A. Senin, A. A. Soldatov, and A. N. Yudin, Phys. Rev. Lett. **115**, 165304 (2015).
[3] V. V. Dmitriev, A. A. Soldatov, and A. N. Yudin, Phys. Rev. Lett. **120**, 075301 (2018).
[4] J. A. Sauls, Phys. Rev. B **88**, 214503 (2013); I. A. Fomin, J. Exp. Theor. Phys. **118**, 765 (2014).
[5] I. A. Fomin, J. Exp. Theor. Phys. **127**, 933 (2018).
[6] P. W. Anderson, J. Phys. Chem. Sol. **11**, 26 (1959).
[7] V. V. Dmitriev, M. S. Kutuzov, A. A. Soldatov, and A. N. Yudin, JETP Lett. **110**, 734 (2019).
[8] V. B. Eltsov, T. Kamppinen, J. Rysti, and G. E. Volovik, arXiv:1908.01645.
[9] A. A. Abrikosov, L. P. Gor'kov, and I. E. Dzyaloshinski, *Methods of Quantum Field Theory in Statistical Physics* (Dover, New York, 1963), Sec. 39.3.
[10] E. V. Thuneberg, S. K. Yip, M. Fogelstrom, and J. A. Sauls, Phys. Rev. Lett. **80**, 2861 (1998).
[11] R. Ikeda, Phys. Rev. Lett. **82**, 3378 (1999); W. Gob, W. Liebich, W. Lang, I. Puica, R. Sobolewski, R. Rossler, J. D. Pedarnig, and D. Bauerle, Phys. Rev. B **62**, 9780 (2000).
[12] M. Tange and R. Ikeda, Phys. Rev. B **101**, 094512 (2020).
[13] S. Yang and R. Ikeda, J. Phys. Soc. Jpn. **83**, 084602 (2014).
[14] D. Volhardt and P. Wolfle, *The Superfluid Phases of Helium 3* (Taylor & Francis, London, 2003).
[15] A. M. Zimmerman, M. D. Nguyen, J. W. Scott, and W. P. Halperin, Phys. Rev. Lett. **124**, 025302 (2020).
[16] N. Nagamura and R. Ikeda, Phys. Rev. B **98**, 094524 (2018).
[17] The corresponding gradient energy within the Ginzburg-Landau approach is already available in Ref. [12].
[18] H. Fukuyama, H. Ebisawa, and S. Maekawa, J. Phys. Soc. Jpn. **53**, 3560 (1984); M. V. Sadovskii, Phys. Rep. **282**, 225 (1997).
[19] L. Andersen, A. Ramires, Z. Wang, T. Lorenz, and Y. Ando, Sci. Adv. **6**, eaay6502 (2020).
[20] D. C. Cavanagh and P. M. R. Brydon, Phys. Rev. B **101**, 054509 (2020).
[21] E. I. Timmons, S. Teknowijoyo, M. Kończykowski, O. Cavani, M. A. Tanatar, S. Ghimire, K. Cho, Y. Lee, L. Ke, N. Hyun Jo, S. L. Bud'ko, P. C. Canfield, P. P. Orth, M. S. Scheurer, and R. Prozorov, arXiv:2001.04673.